Changes in Electroencephalography signals in a juvenile female Fragile X Syndrome mouse model

Authors: Asim Ahmed [1,2,3], Veronica Rasheva [1,2,3], MoonYoung Bae[1,2,3], Kartikeya Murari [1,4,5], Ning Cheng [1,2,3]

Affiliations:

1. Faculty of Veterinary Medicine, University of Calgary, Calgary, AB, Canada.
2. Hotchkiss Brain Institute, Cumming School of Medicine, University of Calgary, Calgary, AB, Canada.
3. Alberta Children's Hospital Research Institute, Cumming School of Medicine, University of Calgary, Calgary, AB, Canada.
4. Department of Biomedical Engineering, Schulich School of Engineering, University of Calgary, Canada.
5. Department of Electrical and Software Engineering, University of Calgary, Calgary, AB, Canada

Abstract:

Background: Fragile X syndrome (FXS) is the leading monogenic cause of Autism. Seizures, hyperactivity, and anxiety are common symptoms of FXS. No broadly effective support option currently exists for FXS, and drug development has suffered many failures in clinical trials based on promising preclinical findings. Thus, effective translational biomarkers of treatment outcomes are needed. Recently electroencephalography (EEG) has been proposed as a translational biomarker in FXS. Being X-linked, FXS is more prevalent in males than females, and there exist significant phenotype differences between males and females with FXS. Recent studies involving male FXS participants and rodent models have identified an increase in absolute gamma EEG power, while alpha power is found to be either decreased or unchanged. However, there is not enough research on female FXS patients or models. In addition, studying EEG activity in young FXS patients or rodent models is crucial for better understanding of the disorder's effects on brain development. Therefore, we aim to compare EEG signal between wild-type (WT) and *fmr1* knockout (KO) female mice at the juvenile stage.

Methods: Frontal-parietal differential EEG was recorded using a stand-alone Open-Source Electrophysiology Recording system for Rodents (OSERR). EEG activity was recorded in three different conditions: a) in the subject's home cage and in the arenas for b) light and dark test and C) open field test. Absolute and relative EEG power as well as phase-amplitude coupling were computed for each condition.

Results: In our study, we found absolute alpha, beta, and gamma EEG power is increased in female *fmr1 KO* mice compared to WT controls at the juvenile age. Alongside, relative theta power is decreased in the *fmr1 KO* females. Furthermore, phase-amplitude coupling is increased in the *fmr1 KO* females.

Discussion and Conclusion: Comparing to the reported changes in EEG signal in male FXS patients and models, our results indicated the presence of sex-based differences in EEG phenotypes at the

juvenile stage. Collectively, these findings suggest that sex is an importance factor to consider in utilizing EEG as a translational biomarker in FXS.

Keywords: Fragile x syndrome, autism, mouse model, Electroencephalography, sex difference, juvenile, neurodevelopment

List of Abbreviations Used (if any):

FXS: Fragile X Syndrome

FMR1: Fragile X Messenger Ribonucleoprotein 1

FMRP: Fragile X Messenger Ribonucleoprotein 1

EEG: Electroencephalography

KO: Knockout

WT: Wildtype

PAC: Phase-amplitude coupling

Introduction and Background:

Autism is one of the most common neurodevelopmental disorders worldwide (1,2). The leading monogenic cause of autism and intellectual disability is fragile X syndrome (FXS). The fragile X messenger ribonucleoprotein (FMRP), encoded by the *fmr1* gene, is lost due to mutations in FXS (3,4). It is estimated to occur 1 in 4,000 males and 1 in 7,000 females (5). Common symptoms include seizures, hyperactivity, and anxiety (6). There is no treatment for autism or FXS, and numerous clinical trials of drugs based on promising preclinical results have failed (7-10). Therefore, it is necessary to develop accurate translational biomarkers, allowing for more fruitful clinical tests and translational success.

Recently, electroencephalogram (EEG) has been identified as a potential translational biomarker of neurodevelopmental disorders, as it can record neural activity across brain regions similarly in humans and animals (7-11). Notably, spontaneous EEG data from male FXS patients and rodent models indicate increased power in the gamma band (12). Therefore, increased gamma power is suggested to be a transferrable hallmark across FXS patients and animal models.

EEG is a method of *in vivo* electrophysiological recording, and it measures electrical activity from the cerebral cortex. EEG signals are generated by the collective electrical activity of neurons in the brain, especially due to the synaptic activity of cortical pyramidal neurons. The rhythmic and synchronized firing of large groups of neurons leads to detectable electrical potentials on the scalp, captured by electrodes. This process involves the spatial summation and temporal coherence of neural oscillations (13). EEG bands comprised of low-frequency bands including delta (1-4Hz), theta (4-8Hz), and alpha (8-12Hz); and high-frequency bands, beta (13-30Hz), and Gamma (30-100 Hz) (14). The slow waves of the low-frequency bands are essential for long-distance or

interregional communication, whereas the fast waves of the high-frequency bands are important for short-distance or intraregional communication (14).

The *fmr1* knockout (KO) mouse model has been employed for over two decades as a fundamental preclinical model for studying FXS (15). The absence of the FMRP protein in these mice leads to changes in neuronal structure, such as altered spine shape and density (16,17), as well as behavioral phenotypes including heightened activity and increased sensitivity to sensory inputs (18,19).

Being an X-linked disorder, FXS is more prevalent in males compared to females (4,5). Females also have FXS, but homozygous mutation is rare. Heterozygous mutation in females manifests milder symptoms, possibly due to skewed X chromosome inactivation (1). In adult FXS patients, male and female participants show an increase in baseline gamma and theta power and decrease in alpha power in EEG (12). Another study in FXS adult patients reported an alteration in theta and low beta power were similar across both sexes, however, relative power varied by sex in the alpha, upper beta, gamma, and epsilon frequency bands (26). In mouse models, male mice also show an increase in spontaneous gamma power in both juvenile and adult age (24). In rat models, adult *fmr1 KO* males showed reduced alpha power and increased gamma power (20).

In general, there is very limited research with female models. One study with adult female *fmr1 KO* mice on B6 background reported no difference in gamma EEG power compared to wildtype controls. However, findings in other frequency bands are not reported (23). Another study in adult female *fmr1 KO* rats found decreased relative theta power (27). Therefore, understanding of the EEG phenotypes in rodent models of FXS has been incomplete, especially regarding females and developmental changes.

In the current study, our objective is to investigate EEG phenotypes in the female *fmr1 KO* mouse model at the juvenile stage. To this end, we conducted EEG recordings from juvenile female mice (at postnatal day 40, P40) and compared *fmr1 KO* and WT genotypes. Our results indicate absolute alpha, beta, and gamma EEG power is increased in *fmr1 KO* female mice compared to WT controls. Alongside, relative theta power is decreased in KO females. Furthermore, phase-amplitude coupling is increased in KO females.

Materials and Methods:

Animals:

Breeder wildtype (FVB.129P2-Pde6b+ Tyrc-ch/AntJ, Jax stock No: 002848) and *fmr1* knockout (*fmr1 KO*-fmr-tm1Cgr, FVB.129 Jax stock No: 004624) mice were obtained from the Jackson Laboratory (ME, USA) and maintained at the mouse facility of the Cumming School of Medicine, University of Calgary. Behavioral testing was performed on female *fmr1 KO* and WT mice, bred in our animal facility at the University of Calgary. All *fmr1 KO* mice of the current study were generated by mating *fmr1 KO* (fmr1 -/-) homozygous females and *fmr1 KO* (fmr1 -/y) males. Mice were group housed (up to five per cage) with their same-sex littermates. The cages were in a room with a controlled 12-hr light-dark cycle (lights on at 7:00am) with access to food and water ad libitum. Mouse pups were weaned around 20 days of age. All mice were fed standard mouse chow (standard diet). Behavioral testing was performed between 09:00h and 19:00h. All behavioral

testing procedures were performed in accordance with the guidelines in the Canadian Council for Animal Care and was approved by the Health Sciences Animal Care Committee of the University of Calgary.

Ethics:

All procedures in this study were performed in accordance with the recommendations in the Canadian Council for Animal Care. The protocol of this study was approved by the Health Sciences Animal Care Committee of the University of Calgary.

EEG surgery, recording and Data analysis:

EEG surgery was carried out in mice utilizing established techniques (11, 28, 29). Mice were given 5% isoflurane to initiate anesthesia, which was subsequently sustained with 1%–2% isoflurane. Mice were placed on top of a heated heating pad on the stereotaxic equipment. The eyes were covered with eye gel to keep them from drying out. After shaving, the scalp was cleaned with 70% ethanol and iodine. Once it was determined that there was no pinch reflex in the toes, the top layer of skin was removed, and the muscles and connective tissue were carefully pushed aside to reveal the skull. To ensure no connective tissue is left, the skull was further cleaned by hydrogen peroxide. To obtain differential frontal-parietal recordings, three small holes were drilled into the skull. The following coordinates were used to fix the electrodes into the holes: ground (AP: +2.5 mm, ML: +1.3 mm), left parietal cortex (AP: −2.2 mm, ML: −2.5 mm), and reference electrode, which is the left frontal cortex (AP: +2.5 mm, ML: −1.3 mm, relative to bregma). After connecting the electrodes to a miniature connector, dental cement was used to affix the assembly to the skull. Following surgery, mice were given analgesic medication and kept on the heating pad until they showed signs of ambulation. EEG recording was conducted 5-7 days following the surgery (Figure 1A). After being briefly sedated with isoflurane inhalation, the subject mouse was connected to stand-alone EEG equipment (11) and then returned to its home cage for EEG recording. A 30-minute recording session in the home cage was followed by a 30-minute recording session in the Light-Dark test chamber. Next day, the same recording was conducted except that the home cage recording was followed by recording in the Open Field test chamber (Figure 1B).

Light-dark test: The apparatus consists of a dark and a brightly lit compartment. The subject was free to move between the two compartments during the 10 minutes test (30).

Open field test: A subject was placed in an empty square shaped chamber and monitored for 10 minutes under room light (3).

Standard procedures were followed for the analysis of EEG data (28, 29). The recording quality was assessed (Figure 1C), and a 5-minute EEG segment at the end of each condition (home cage, Light-Dark, and Open Field Test) was chosen for analysis. Additionally, we ensured that mice remained awake during these EEG segments. Using MATLAB, Welch's approach (31) was used to compute the power spectral density (PSD) of the EEG signal. We divided the EEG data into 2-second epochs. A Hamming window was used to compute periodograms for each epoch, and then averaged to get the final PSD estimate at a 0.5 Hz spectral resolution. To determine the power in each of the following frequency bands: delta (1–4 Hz), theta (4–8 Hz), alpha (8–13 Hz), beta (13–30 Hz), and gamma (30–100 Hz), the PSD was integrated using the trapezoidal technique. Two sub-divisions were made for

the gamma band: "low gamma (30–60 Hz)" and "high gamma (60–100 Hz)." Furthermore, a Fast-Fourier Transform was used to compute a continuous power spectrum, which was displayed on a decibel scale (10*log10). Relative power was calculated as the ratio of the power of a particular band to the total power of all bands summed together.

Phase-amplitude cross-frequency coupling (PAC) was measured by further analysis of the EEG data. The PAC between gamma band (30–100 Hz) and lower frequency oscillations (4–12 Hz) was measured using a time-frequency based approach (33). This quantified the modulation of the amplitude of gamma oscillation with the phase of the slow rhythm. Using the RID-Rihaczek distribution, the high frequency oscillation's envelope and the low frequency oscillation's phase were obtained. The extracted amplitude and phase time series were then used to compute the mean vector length (MVL), which was used to quantify PAC. MVL measures the circular variances by measuring the complex composite signal's mean magnitude. It is a modulation index used to measure the modulation between the phase and amplitude time series (32). Two minutes of spontaneous EEG activity were examined. Using a step of 1 Hz for low frequencies (referred to as "phase frequency") and a step of 2 Hz for high frequencies (referred to as "amplitude frequency") from intervals of 30–100 Hz, MVL was computed.

Statistical tests and analysis:

The sample size was determined based on previous reports and preliminary data. For EEG recording, animals with noisy signals, which had much larger and often saturating amplitudes than the real signal and were likely due to connection issues from the constructed electrodes to the connector after the surgery, were excluded from the analysis. Sample size n means number of individual animals used. Unpaired student's t-test (assuming two-tailed distribution and two-sample unequal variance) or Mann-Whitey U test was used to compare EEG signal between WT and *fmr1 KO* for absolute and relative power as well as PAC. Values are mean± SEM. Levels of significance are: *: $p < 0.05$, **: $p < 0.0l$, ***: $p < 0.001$.

Results:

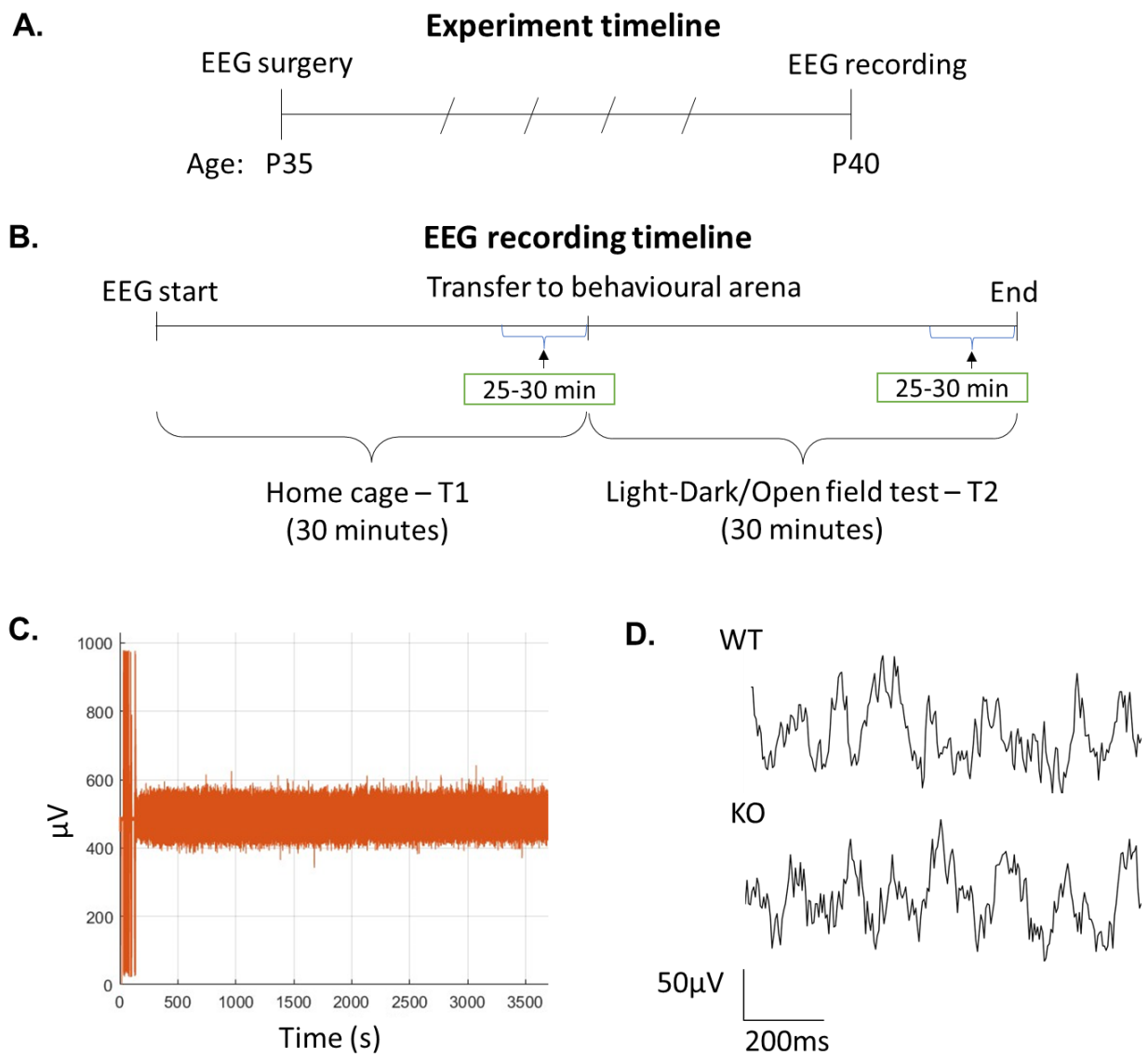

Figure 1: Experimental timeline and EEG recording timeline. (A) Experimental timeline, with EEG surgery at P35 and EEG recording at P40. (B) EEG recording timeline; first 30 minutes of EEG recording was in the home cage and, the next 30 minutes was in the behavioral arena. For analysis, we only used the last 5 minutes (25-30 minutes) of EEG recordings from the home cage and behavioral arena. (C) EEG raw signal from 1 hour of recording. The noise in the first 120 seconds (about 2 minutes) shows the time when the mice is anesthetized, and the EEG recording device is connected on mouse head cap. (D) Example of EEG signal.

Absolute alpha, beta and gamma EEG power is increased in *fmr1 KO* female mice compared to WT controls.

Power spectra indicated that EEG power is increased in *fmr1 KO* mice compared to WT controls in the frequency range of alpha, beta, and gamma (8-100Hz) in home cage (A), light-dark test arena (B) and open field test arena (C). In home cage recording (D), we observed that absolute EEG power in alpha, beta, and gamma, including low and high gamma frequency bands, is increased in *fmr1 KO* female mice compared to WT controls. Alongside, total power is also increased in the KO mice. However, absolute EEG power in delta and theta bands was similar between *fmr1 KO* and WT mice. Similar increases in alpha, beta, gamma, including low and high gamma bands, and total EEG power were found in light-dark test and open field test recordings, as summarized in Table 1. Therefore, it is evident that EEG power is consistently increased in the female *fmr1 KO* mice in the frequency range of 8-100Hz, compared to WT controls, regardless of the three testing conditions used.

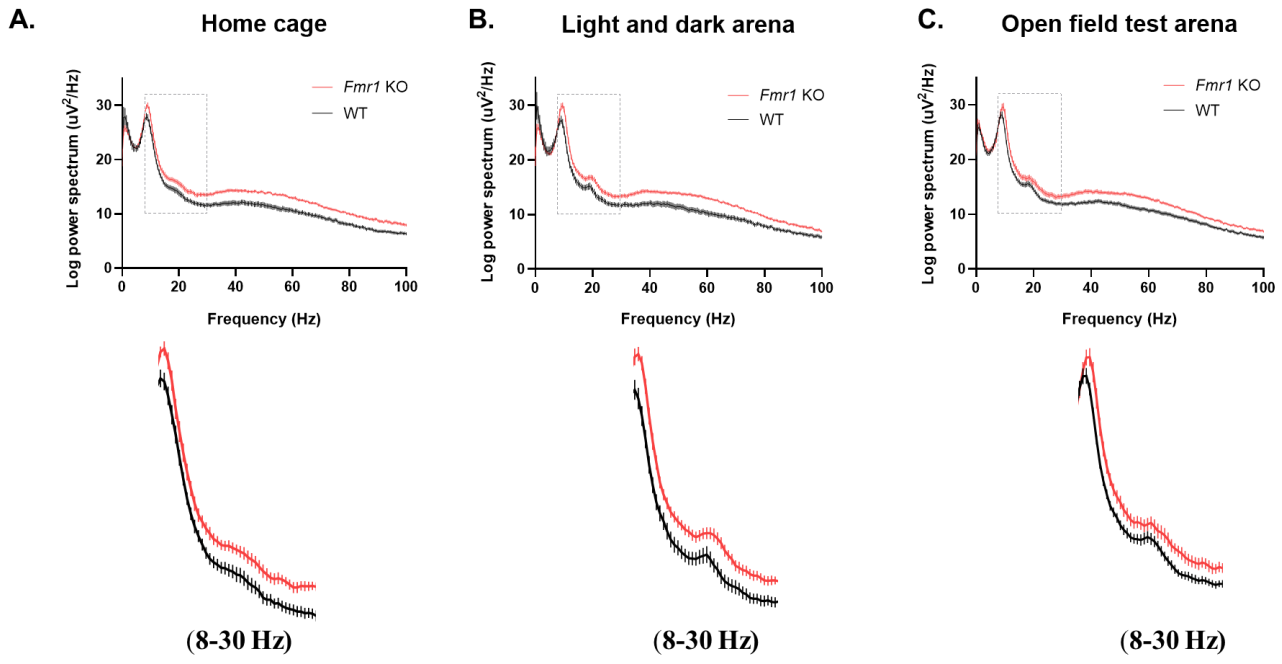

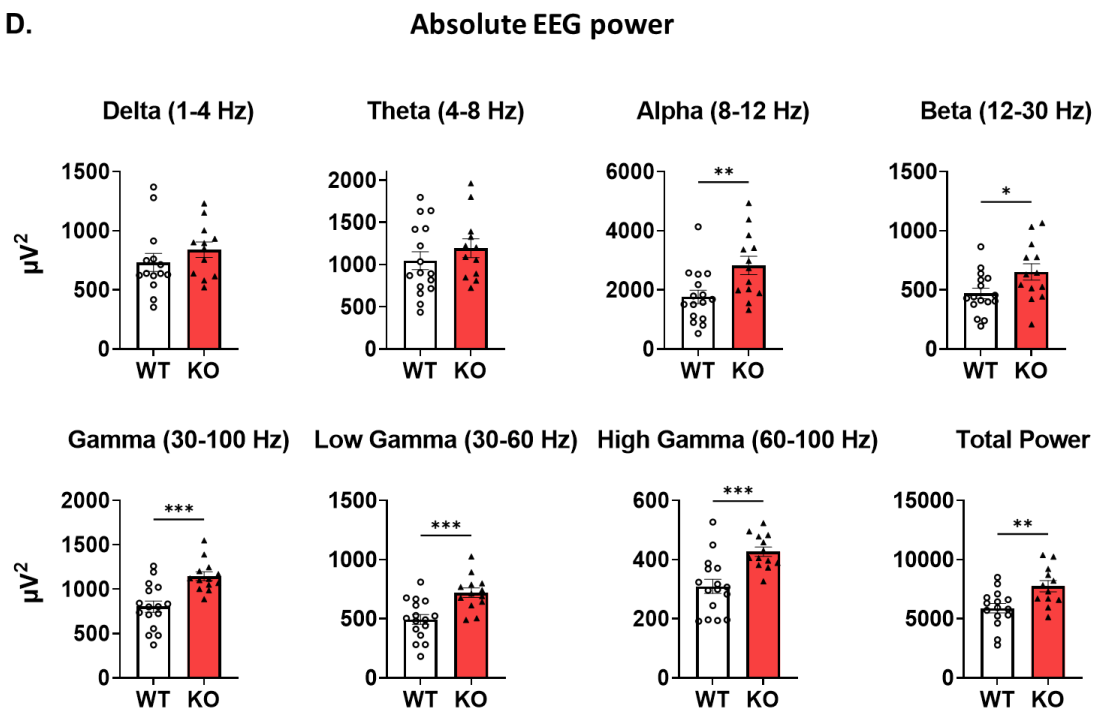

Figure 2: Alpha, beta, and gamma power is increased in KO compared to WT mice. (A, B, & C) Power spectra of KO (n=11) and WT (n=14) female mice in the home cage, light-dark test, and open field test arena. (D) Comparison of absolute EEG power between WT and KO, in delta, theta, alpha, beta, and gamma, low and high gamma frequency band, and total power in home cage recordings (Student's t-test). Values are mean ±SEM. *: P < 0.05, **: P < 0.01, ***: P < 0.001. Detailed descriptions of statistical analysis methods are presented in Methods.

Table 1: P-value summary of comparing absolute EEG power in light-dark and open field test arenas between female *fmr1 KO* and WT mice.

Frequency bands	Light-dark test arena	Open field test arena
Delta	0.2311	0.4231
Theta	0.9567	0.2680
Alpha ↑	**0.0260**	**0.0076**
Beta ↑	**0.0292**	**0.0049**
Gamma ↑	**0.0003**	**<0.0001**

Low gamma ↑	**0.0007**	**0.0001**
High gamma ↑	**0.0006**	**<0.0001**
Total EEG power ↑	**0.0111**	**0.0026**

Table 1: Summary of the P-vales from Student's t-test between *fmr1 KO* and WT mice when comparing absolute EEG power in light-dark and open field test arenas. Arrowhead and bold text indicate significant increase in power in *fmr1 KO* mice compared to WT controls.

Relative theta EEG power is decreased in *fmr1 KO* female mice compared to WT controls.

In home cage recording, there is no change in relative EEG power between *fmr1 KO* female mice and WT controls (Figure 3). Interestingly, in light-dark and open field test, we found a decrease in relative theta power in *fmr1 KO* female mice compared to WT controls (Table 2).

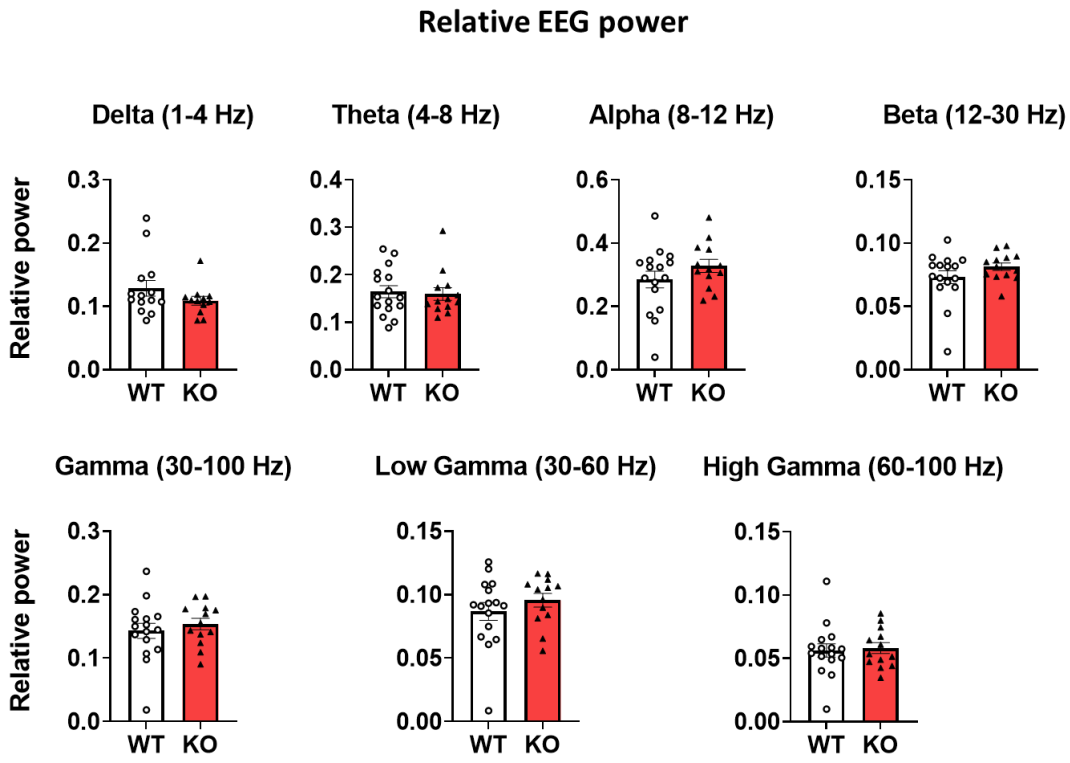

Figure 3: No difference is observed in relative EEG power between KO and WT females in home cage recording. Figure shows relative EEG power for delta, theta, alpha, beta, and gamma including low and high gamma in home cage recording. Relative power is computed by dividing individual band EEG power from the total power. Sample size: KO (n=11) and WT (n=14) (Student's t-test). Values mean ± SEM. Detailed descriptions of statistical analysis methods are presented in Methods.

Table 2: P-value summary of relative EEG power from light dark and open field test arenas

Frequency bands	Light- dark test arena	Open field test arena
Delta	0.0823	0.1245
Theta ↓	**0.0009**	**0.0002**
Alpha	0.1563	0.0632
Beta	0.3079	0.2887
Gamma	0.4488	0.2803
Low gamma	0.3744	0.2618
High gamma	0.4453	0.4118

Table 2: It summarizes the P-vales from Student's t-test between KO and WT relative EEG power recorded in light-dark and open field test arenas. Arrowhead and bold text show a significant decrease in relative power in KO as compared to WT controls.

Increased phase-amplitude coupling in *fmr1 KO* female mice compared to WT controls:

In addition, we investigated phase-amplitude coupling (PAC) in the recorded EEG signal. The most researched kind of cross-frequency coupling, or PAC, explains how oscillations in the brain network interact with one another at various frequency ranges (34-39). PAC measures how the phase of a lower frequency oscillation (referred to as "phase frequency") modulates the amplitude of a high frequency oscillation (referred to as "amplitude frequency"). It has been suggested that it functions as a mechanism for integrating large-scale neural networks by synchronizing neuronal firing time, which is necessary for efficient information processing (40-42). Furthermore, earlier research reported that children with autism have greater alpha to gamma PAC strength as compared to typically developing controls (43, 50). Our analysis shows that in-home cage, as well as light-dark test and open-field test arenas, the strength of PAC, measured between the amplitude of gamma band (30–100 Hz) and the phase of lower frequency oscillations (4–12 Hz), is higher in KO female mouse models compared to WT controls (Figure 4: A, B, and C).

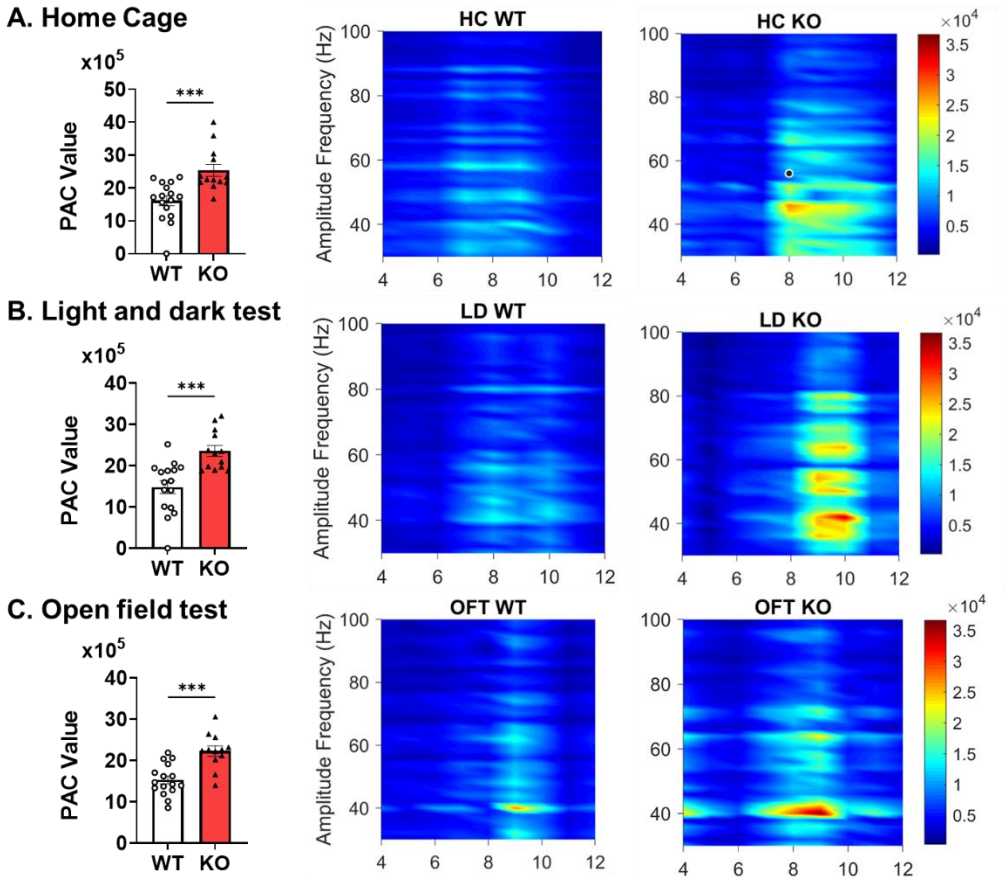

Figure 4: Phase-amplitude coupling is increased in KO mice compared to WT controls. (A, B, & C) shows the quantification of phase amplitude coupling and phase amplitude map for recordings in home cage, light-dark, and open filed test arenas. The left panels show the quantification of total mean vector length (MVL) values and comparison between WT and KO female mice. The right panel shows representative phase-amplitude map between the amplitude of the gamma band (30 – 100 Hz, amplitude-frequency) and the phase of the low-frequency band (4 – 12 Hz, phase frequency). The color scale is representative of MVL values, a measurement of PAC. WT (n = 14) and KO (n = 11) (Student's t-test). Values are mean ± SEM. ***: $p < 0.001$. Detailed descriptions of statistical analysis methods are presented in Methods.

Table 3: Summary of EEG phenotypes across different study models, including sex and developmental age differences

Sex and developmental age differences in resting state EEG phenotypes across different studied models:		
FXS patients	**Children**	
	Males	**Females**
	?	?
	Adults	

	Males	Females
	• Increased relative power in theta and gamma bands, but decreased power in low and high alpha bands (12) • Increased relative theta power and decreased relative upper-alpha power (Gamma power is not reported) (21)	• Increased relative power in theta and gamma bands, but reduced power in low and high alpha bands (study had small sample size) (12)
***fmr1 KO* mice**	**Juveniles**	
	Males	**Females**
	• Increased absolute gamma EEG power (B6 background) (22) • Increased absolute gamma EEG power (FVB background) (24)	• Increased absolute alpha, beta, and gamma EEG power (FVB background) (present study) • Decrease in relative theta power (FVB background) (present study)
	Adults	
	Males	**Females**
	• Increased absolute gamma EEG power (FVB background) (24) • Increased absolute and relative gamma EEG power (B6 background) (23)	• No change in absolute or relative gamma EEG power (B6 background, findings in other frequency bands were not reported) (23)
***fmr1 KO* rats**	**Juvenile**	
	Males	**Females**
	• Increased relative EEG power in frequency range (18–52 Hz) and decreased relative EEG power in the frequency range (3–9 Hz) (both male and female) (62)	• Increased relative EEG power in frequency range (18–52 Hz) and decreased relative EEG power in the frequency range (3–9 Hz) (both male and female) (62)
	Adult	
	Males	**Females**
	• For absolute EEG, gamma power is increased, and alpha power is reduced (20) • For relative EEG, gamma power is increased, and alpha-beta power is decreased (20)	• Decreased relative theta EEG power (27)

	• Increased relative gamma EEG power (27)	

Discussion:

EEG as a translational biomarker for FXS.

As we know, currently no cure exists for FXS, and many drugs have failed in numerous clinical trials. Thus, there is a need for an effective translational biomarker (7-10). EEG has been suggested as such a biomarker for FXS, with potential indicators identified in the EEG abnormalities observed in FXS patients. These include elevated gamma power at rest, reduced gamma phase-locking in sensory cortices, and increased amplitudes of event-related potentials. Such deviations could signal cortical hyperactivity, which may result from a disruption in the balance between excitatory systems, driven by glutamate, and inhibitory systems, mediated by GABA, in FXS (8).

Although the exact underlying mechanisms generating gamma oscillation are still being debated, the inhibitory GABAergic interneurons have been proposed to play a critical role in synchronizing cortical activities at gamma frequencies (44-46). Additionally, dysfunctional inhibitory neurons and associated circuits have been identified in the rodent models of Fragile X Syndrome, which lead to impaired inhibitory control of cortical synchronization (47-49).

There is some evidence from clinical trials showing that treatment-related changes in EEG may be associated with clinical improvements (7). However, these findings require replication and extension to other medications. While the use of EEG characteristics as biomarkers is still in the early phases, the current research is promising and signals the emergence of an effective translational biomarker (7).

Increased PAC in KO as compared to WT:

Cross-frequency coupling has been developed as a method to assess moment-to-moment interaction between oscillations of different frequencies within EEG signals (50). PAC assesses how the amplitude of high-frequency activity is modulated by the phase of low-frequency oscillations. In the brain, strong coupling functions as a clocking mechanism to produce perceptual windows that, in turn, integrate and separate temporally relevant and irrelevant information (51). Since the phase and frequency of the PAC vary depending on the cortical layer (52, 53), it is hypothesized that they represent the top-down vs bottom-up direction of information flow in the cortex (54-56). The equilibrium of top-down and bottom-up processing in the cortex could indicate how sensory information is processed and anticipated. This is especially relevant to autism (54-57) because autism is often associated with difficulties in predicting sensory input and challenges in developing executive functions (56).

A recent EEG study comparing children with autism and typically developing controls, aged 6-11 years identified a notable increase in alpha-gamma and theta-gamma PAC strength in the autism group. Additionally, the study revealed significant correlations between whole-brain theta-gamma PAC strength with autism severity scores on social communication abilities, IQ and levels of restricted and repetitive behaviors across both cohorts (50). This is consistent with our results

from FXS mouse model, where the strength of PAC, measured between the amplitude of the gamma band and the phase of lower frequency oscillations (4–12 Hz), is higher in KO female mouse models compared to WT controls. This increase in PAC strength in KO mice may point to modifications in neural network integration processes by reflecting a changed dynamic in the interplay between various frequency oscillations.

Another study using magnetoencephalography studied the relationship between the PAC and the severity of autism symptoms in specific brain regions. They highlighted autism specific abnormalities in alpha to low-gamma PAC, with increased PAC in central midline areas and decreased PAC in lateral areas (58). Significantly, increased PAC strength correlated with poorer social communication, as measured by higher social responsiveness scale scores, across both autism and typically developing control participants. This correlation did not persist within the autism group alone. Thus, the authors suggested PAC's potential as a biomarker requires further investigation for autism-specific clinical utility. (58).

Sex differences in EEG studies in FXS mouse models:

For EEG to be a reliable biomarker, it is crucial to determine its phenotypic consistency across sexes, developmental stages, and various study models. Table 3 summarizes the different studies that have evaluated the EEG phenotypes across different study models including humans, rats, and mice. Overall, increased gamma power in both absolute and relative EEG across patients and rodent models in both sexes have been observed (Table 3). Regarding females, one study reported that adult FXS patients showed increase in relative theta power. In contrast, rat and mouse models reported a decrease in relative theta power. Thus, there are opposite changes in the theta frequency range between female FXS patients and rodent models (Table 3). However, it should be noted that research on female FXS patients is limited, with relatively small sample sizes (12). Alongside, a few studies have mentioned that neurotypical women exhibit greater resting state total EEG power compared to neurotypical men (59-61). Such gender-specific variations in EEG phenotypes are clinically significant, indicating potential differences in the impact of low-frequency modulation on gamma power between genders (28). Overall, there is a pressing need for further research involving female FXS patients to enhance our understanding of how gender, symptom severity, and changes in EEG interrelate.

Regarding *fmr1 KO* rat model of FXS, one study did not observe sex-specific EEG phenotypes in juvenile rats, as both male and female *KO* rats have increased relative EEG power in frequency range of 18-52 Hz and decreased relative EEG power in frequency range of 3-13 Hz (62). However, another study in adult *fmr1 KO* rats did reveal a sex-specific EEG phenotype, as male KO rats exhibited an elevation in relative gamma EEG power, while female KO rats exhibited decrease in relative theta power and no change in gamma power (27).

For mouse models, male mice show an increase in absolute gamma EEG power in both juvenile and adult ages, in both FVB and B6 background (22-24). In our current study, juvenile *fmr1 KO* female mice on the FVB background show an increase in absolute alpha, beta and gamma EEG power. Therefore, we conclude that there is sex-based EEG phenotypic difference in juvenile mice with FVB background. However, there is no available study on adult female FXS mouse model with FVB background, to further validate if sex differences exist in adult mice. Future EEG studies focusing on

adult female FXS mouse model are essential. Such research will substantially enhance our comprehension of EEG phenotypes in FXS mouse models, encompassing aspects of both sex and age. Interestingly, one study on adult *fmr1 KO* female mice on the B6 background reported no change in absolute or relative gamma EEG power (23). Therefore, while choosing the FXS mouse model, we should consider the background strain of mice, as well as their sex and developmental stage, as EEG phenotypes could depend on these variables.

Author's contribution:

AA participated in EEG surgery, recording, data analysis and interpretation, and drafted and revised the manuscript. VR participated in EEG surgery, recording, data analysis and interpretation. MB participated in EEG recording. KM participated in data analysis and interpretation. NC designed the study, participated in data analysis and interpretation, and revised the manuscript. All authors read and approved the final manuscript.

Funding statement:

This work was supported by the Alberta Children's Hospital Research Foundation (NC), University of Calgary Faculty of Veterinary Medicine (NC), Natural Sciences and Engineering Research Council of Canada (NC), and FRAXA Research Foundation (NC). The funding sources had no role in the study design; in the collection, analysis, and interpretation of data; in the report's writing; and in the decision to submit the article for publication.

References:

1. Lord, C. et al. autism spectrum disorder. Nature Reviews Disease Primers 6, 5 (2020).
2. DiCicco-Bloom, E. et al. The developmental neurobiology of autism spectrum disorder. J. Neurosci. 26, 6897 6906 (2006).
3. Zhan, X. et al. FMRP (1-297)-tat restores ion channel and synaptic function in a model of Fragile X syndrome. Nat. Communication. 11, 2755 (2020).
4. Bagni, C., Tassone, F., Neri, G. & Hagerman, R. Fragile X syndrome: causes, diagnosis, mechanisms, and therapeutics. J. Clin. Invest. 122, 4314 4322 (2012).
5. Hagerman RJ, Berry-Kravis E, Hazlett HC, Bailey DB Jr, Moine H, Kooy RF, et al. Fragile X syndrome. Nat Rev Dis Primers. 2017 Sep 29; 3:17065.
6. Razak, K.A., Dominick, K.C. & Erickson, C.A. Developmental studies in fragile X syndrome. *J Neurodevelop Disord* 12, 13 (2020). https://doi.org/10.1186/s11689-020-09310-9
7. Sahin, M. et al. Discovering translational biomarkers in neurodevelopmental disorders. Nat. Rev. Drug Discov. (2018) doi:10.1038/d41573-018-00010-7.
8. Kenny, A., Wright, D. & Stanfield, A. C. EEG as a translational biomarker and outcome measure in fragile X syndrome. Transl. Psychiatry 12, 34 (2022).
9. Ewen, J. B., Sweeney, J. A. & Potter, W. Z. Conceptual, Regulatory and Strategic Imperatives in the Early Days of EEG- Based Biomarker Validation for Neurodevelopmental Disabilities. Front. Integr. Neurosci. 13, 45 (2019).
10. Featherstone, R. E. et al. EEG biomarkers of target engagement, therapeutic effect, and disease process. Ann. N. Y. Acad. Sci. 1344, 12¿26 (2015).

11. Cheng, N. & Murari, K. OSERR: an open-source standalone electrophysiology recording system for rodents. Sci. Rep. 10, 16996 (2020).
12. Wang, J. et at. A resting EEG study of neocortical hyperexcitability and altered functional connectivity in fragile X syndrome. J. Neurodev. Disord. 9, 11 (2017).
13. Buzsáki, G., Anastassiou, C. & Koch, C. The origin of extracellular fields and currents — EEG, ECoG, LFP and spikes. Nat Rev Neurosci 13, 407–420 (2012). https://doi.org/10.1038/nrn3241
14. Buzsáki G, Draguhn A. Neuronal oscillations in cortical networks. Science. 2004; 304:1926–9.
15. Dahlhaus, R. Of men and mice: modeling the fragile x syndrome. Front. Mol. Neurosci. 11, 41. *https://doi.org/10.3389/fnmol* .2018.00041 (2018).
16. Till, S. M. et al. Conserved hippocampal cellular pathophysiology but distinct behavioural defcits in a new rat model of FXS. Hum. Mol. Genet. 24, 5977–5984. https://doi.org/10.1093/hmg/ddv299 (2015).
17. Grossman, A. W., Elisseou, N. M., McKinney, B. C. & Greenough, W. T. Hippocampal pyramidal cells in adult fmr1 knockout mice exhibit an immature-appearing profile of dendritic spines. Brain Res. 1084, 158–164. https://doi.org/10.1016/j.brainres.2006.02.044 (2006).
18. Kazdoba, T. M., Leach, P. T., Silverman, J. L. & Crawley, J. N. Modeling fragile X syndrome in the fmr1 knockout mouse. Intract. Rare Dis. Res. 3, 118–133.
19. Lovelace, J. W., Ethell, I. M., Binder, D. K. & Razak, K. A. Translation-relevant EEG phenotypes in a mouse model of Fragile X Syndrome. Neurobiol. Dis. 115, 39–48. https://doi.org/10.1016/j.nbd.2018.03.012 (2018).
20. Kozono, N., Okamura, A., Honda, S. et al. Gamma power abnormalities in a fmr1-targeted transgenic rat model of fragile X syndrome. Sci Rep 10, 18799 (2020). https://doi.org/10.1038/s41598-020-75893-x
21. Van der Molen, M. J. & Van der Molen, M. W. Reduced alpha and exaggerated theta power during the resting-state EEG in fragile X syndrome. Biol. Psychol. 92, 216–219. https://doi.org/10.1016/j.biopsycho.2012.11.013 (2013).
22. Lovelace, J. W. et al. Deletion of fmr1 from forebrain excitatory neurons triggers abnormal cellular, EEG, and behavioral phenotypes in the auditory cortex of a mouse model of fragile x syndrome. Cereb. Cortex https://doi.org/10.1093/cercor/bhz141 (2019).
23. Sinclair, D. et al. GABA-B agonist baclofen normalizes auditory-evoked neural oscillations and behavioral deficits in the fmr1 knockout mouse model of fragile x syndrome. eNeuro 4, doi: https://doi.org/10.1523/ENEURO.0380-16.2017 (2017).
24. Wen, T.H., Lovelace, J.W., Ethell, I.M., Binder, D.K., Razak, K.A., 2019. Developmental changes in EEG phenotypes in a mouse model of fragile X syndrome. Neuroscience 398, 126–143.
25. Ethridge LE, De Stefano LA, Schmitt LM, Woodruff NE, Brown KL, Tran M, Wang J, Pedapati EV, Erickson CA, Sweeney JA. Auditory EEG Biomarkers in Fragile X Syndrome: Clinical Relevance. Front Integr Neurosci. 2019 Oct 9; 13:60. doi: 10.3389/fnint.2019.00060. PMID: 31649514; PMCID: PMC6794497.
26. Smith EG, Pedapati EV, Liu R, Schmitt LM, Dominick KC, Shaffer RC, Sweeney JA, Erickson CA. Sex differences in resting EEG power in Fragile X Syndrome. J Psychiatr Res. 2021 Jun;

138:89-95. doi: 10.1016/j.jpsychires.2021.03.057. Epub 2021 Mar 31. PMID: 33836434; PMCID: PMC8192450
27. Wong, H., Hooper, A.W.M., Niibori, Y., Lee, S.J., Hategan, L.A., Zhang, L., KarumuthilMelethil, S., Till, S.M., Kind, P.C., Danos, O., Bruder, J.T., Hampson, D.R., 2020. Sexually dimorphic patterns in electroencephalography power spectrum and autism related behaviors in a rat model of fragile X syndrome. Neurobiol. Dis. 146, 105118.
28. Mayengbam S, Ellegood J, Kesler M, et al. A ketogenic diet affects brain volume and metabolome in juvenile mice. Neuroimage. 2021; 244:118542.
29. Murari K, Abushaibah A, Rho JM, Turner RW, Cheng N. A clinically relevant selective ERK-pathway inhibitor reverses core deficits in a mouse model of autism. EBioMedicine. 2023 May; 91:104565. doi: 10.1016/j.ebiom.2023.104565. Epub 2023 Apr 21. PMID: 37088035; PMCID: PMC10149189.
30. Bourin, M. & Hascoet, M. The mouse light/dark box test. Eur. J. Pharmacol. 463, 55-65 (2003).
31. Welch P. The use of fast Fourier transform for the estimation of power spectra: a method based on time averaging over short, modified periodograms. IEEE Trans Audio Electroacoust. 1967;15:70–73.
32. Canolty, R.T., Edwards, E., Dalal, S.S., Soltani, M., Nagarajan, S.S., Kirsch, H.E., Berger, M.S., Barbaro, N.M., Knight, R.T. "High Gamma Power Is Phase-Locked to Theta Oscillations in Human Neocortex." Science, vol. 313, 2006, pp. 1626-1628.
33. Munia, T.T.K., and S. Aviyente. "Time-Frequency Based Phase-Amplitude Coupling Measure for Neuronal Oscillations." Scientific Reports, vol. 9, 2019, p. 12441.
34. R.T. Canolty, E. Edwards, S.S. Dalal, M. Soltani, S.S. Nagarajan, H.E. Kirsch, M.S. Berger, N. Barbaro, R.T. Knight. High gamma power is phase-locked to theta oscillations in human neocortex Science, 313 (2006), pp. 1626-1628
35. T. Canolty, R.T. Knight. The functional role of cross-frequency coupling Trends Cognit. Sci., 14 (2010), pp. 506-515
36. A. Hyafil, A.-. L. Giraud, L. Fontolan, B. Gutkin. Neural cross-frequency coupling: connecting architectures, mechanisms, and functions Trends Neurosci., 38 (2015), pp. 725-740
37. O. Jensen, L.L. Colgin. Cross-frequency coupling between neuronal oscillations Trends Cognit. Sci., 11 (2007), pp. 267-269
38. V. Jirsa, V. Müller. Cross-frequency coupling in real and virtual brain network. Front. Comput. Neurosci., 7 (2013), p. 78
39. J.E. Lisman, O. Jensen. The theta-gamma neural code. Neuron, 77 (2013), pp. 1002-1016
40. A. Bragin, G. Jandó, Z. Nádasdy, J. Hetke, K. Wise, G. Buzsáki. Gamma (40–100Hz) oscillation in the hippocampus of the behaving rat J. Neurosci., 15 (1995), pp. 47-60.
41. P. Fries. A mechanism for cognitive dynamics: neuronal communication through neuronal coherence. Trends Cognit. Sci., 9 (2005), pp. 474-480
42. A.B.L. Tort, R. Komorowski, H. Eichenbaum, N. Kopell. Measuring phase-amplitude coupling between neuronal oscillations of different frequencies. J. Neurophysiol., 104 (2010), pp. 1195-1210

43. J.I. Berman, S. Liu, L. Bloy, L. Blaskey, T.P.L. Roberts, J.C. Edgar. Alpha-to-gamma phase-amplitude coupling methods and application to autism spectrum disorder. Brain Connect., 5 (2015), pp. 80-90
44. Tamás G, Buhl EH, Lörincz A, Somogyi P. Proximally targeted GABAergic synapses and gap junctions synchronize cortical interneurons. Nat Neurosci. 2000; 3:366–371.
45. Szabadics J, Lorincz A, Tamás G. β and γ frequency synchronization by dendritic GABAergic synapses and gap junctions in a network of cortical interneurons. J Neurosci. 2001; 21:5824–5831.
46. Hasenstaub A, Shu Y, Haider B, Kraushaar U, Duque A, McCormick DA. Inhibitory postsynaptic potentials carry synchronized frequency information in active cortical networks. Neuron. 2005; 47:423–435.
47. Patel AB, Hays SA, Bureau I, Huber KM, Gibson JR. A target cellspecific role for presynaptic fmr1 in regulating glutamate release onto neocortical fast-spiking inhibitory neurons. J Neurosci. 2013; 33:2593–2604.
48. Selby L, Zhang C, Sun QQ. Major defects in neocortical GABAergic inhibitory circuits in mice lacking the fragile X mental retardation protein. Neurosci Lett. 2007; 412:227–232.
49. Paluszkiewicz SM, Olmos-Serrano JL, Corbin JG, Huntsman MM. Impaired inhibitory control of cortical synchronization in fragile X syndrome. J Neurophysiol. 2011; 106:2264–2272. https://doi.org/10. 1152/jn.00421.2011.
50. Fleming Peck, A. J. Naples, S. J. Webb, R. A. Bernier, K. Chawarska, G. Dawson, S. Faja, S. Jeste, M. Murias, C. A. Nelson, F. Shic, C. Sugar, D. Şentürk, J. C. McPartland, & A. R. Levin. (2022). Phase-Amplitude Coupling in Autism Spectrum Disorder: Results from the Autism Biomarkers Consortium for Clinical Trials. bioRxiv.
51. Womelsdorf T, Valiante TA, Sahin NT, Miller KJ, Tiesinga P (2014): Dynamic circuit motifs underlying rhythmic gain control, gating and integration. *Nature Neuroscience* 17: 1031–1039.
52. Sotero RC, Bortel A, Naaman S, Mocanu VM, Kropf P, Villeneuve M, Shmuel A (2015): Laminar Distribution of Phase-Amplitude Coupling of Spontaneous Current Sources and Sinks. Frontiers in Neuroscience 9: 454.
53. Márton CD, Fukushima M, Camalier CR, Schultz SR, Averbeck BB (2019): Signature Patterns for Top-Down and Bottom-Up Information Processing via Cross-Frequency Coupling in Macaque Auditory Cortex. *eneuro* 6: ENEURO.0467-18.2019.
54. Mariscal MG, Levin AR, Gabard-Durnam LJ, Xie W, Tager-Flusberg H, Nelson CA (2021): EEG Phase-Amplitude Coupling Strength and Phase Preference: Association with Age over the First Three Years after Birth. *eneuro* 8: ENEURO.0264-20.2021.
55. Mariscal MichaelG, Berry-Kravis E, Buxbaum JD, Ethridge LE, Filip-Dhima R, Foss-Feig JH, et al. (2021): Shifted phase of EEG cross-frequency coupling in individuals with Phelan-McDermid syndrome. *Molecular Autism* 12: 29.
56. Pellicano E, Burr D (2012): When the world becomes 'too real': a Bayesian explanation of autistic perception. *Trends in Cognitive Sciences* 16: 504–510.
57. Sinha P, Kjelgaard MM, Gandhi TK, Tsourides K, Cardinaux AL, Pantazis D, et al. (2014): Autism as a disorder of prediction. *Proceedings of the National Academy of Sciences* 111: 15220–15225.

58. Port RG, Dipiero MA, Ku M, Liu S, Blaskey L, Kuschner ES, et al. (2019): Children with Autism Spectrum Disorder Demonstrate Regionally Specific Altered Resting-State Phase–Amplitude Coupling. *Brain Connectivity* 9: 425–436.
59. Bao L-Q, Qiu J-L, Tang H, Zheng W-L, Lu B-L. Investigating sex differences in classification of five emotions from EEG and eye movement signals. *Annu Int Conf IEEE Eng Med Biol Soc.* 2019; 2019:6746–9.
60. Flor-Henry P. Observations, reflections and speculations on the cerebral determinants of mood and on the bilaterally asymmetrical distributions of the major neurotransmitter systems. *Acta Neurol Scand Suppl.* 1986; 109:75–89.
61. Matsuura M, Yamamoto K, Fukuzawa H, Okubo Y, Uesugi H, Moriiwa M, et al. Age development and sex differences of various EEG elements in healthy children and adults-quantification by a computerized wave form recognition method. *Electroencephalogr Clin Neurophysiol.* 1985; 60:394–406.
62. Berzhanskaya, J., et al. "Disrupted Cortical State Regulation in a Rat Model of Fragile X Syndrome." *Cerebral Cortex*, vol. 27, 2017, pp. 1386-1400.